Original Paper

Computational Modeling of Network Topology and Molecular Dynamics for the Assessment of Therapeutic Potential of the *Astragalus Membranaceus-Salvia Miltiorrhiza* Drug Pair in the Treatment of Chronic Kidney and Heart Failure

Jiayou Liu,[1] Jianguo Qin[2]*

[1]The Second Clinical Medical College, Beijing University of Chinese Medicine, Beijing 100078, China
[2]Department of Nephropathy, Dongfang Hospital, Beijing University of Chinese Medicine, Beijing100078, China

Keywords. *Astragalus membranaceus-Salvia miltiorrhiza*; Chronic kidney disease; Chronic heart failure; Network pharmacology; Molecular dynamics simulation

Introduction. The bioactive components of *Astragalus membranaceus* and *Salvia miltiorrhiza* improved cardiac and renal function in chronic heart failure (CHF) and chronic kidney disease (CKD), respectively. However, the common regulating molecular mechanisms remain unclear. The aim of this study was to investigate these mechanisms using bioinformatics, network topology, and molecular dynamics simulation techniques.

Methods. The active components and target sites of *A. membranaceus* and *S. miltiorrhiza* were obtained from the Traditional Chinese Medicine Systems Pharmacology database. The targets of CKD and CHF were obtained from various databases for a protein-protein interaction analysis. The Gene Ontology (GO) function and Kyotoencyclopedia of genes and genomes (KEGG) pathway enrichment of intersection targets were analyzed by using the Database for Annotation, Visualization, and Integrated Discovery (DAVID) database. Molecular docking and dynamic simulations were conducted on the core ingredients and targets. The diagnostic efficiency of the key targets was evaluated by using receiver-operating characteristic (ROC) curves.

Results. A total of 70 active ingredients and 158 common targets were found. The top five core targets were AKT1, STAT3, TP53, MAPK1, and RELA. The GO enrichment analysis included apoptosis and oxidative stress. The KEGG pathway enrichment results indicated that the drug pair regulated the AGE-receptor for AGE signaling pathway, fluid shear stress and atherosclerosis, and the IL-17 signaling pathway. Molecular docking and dynamic simulations confirmed that the core ingredients had good affinity and stability with the key targets. The ROC curves confirmed the accuracy of every key target for identifying CKD and CHF and demonstrated that combining them improves diagnosis.

Conclusion. The combination of *A. membranaceus* and *S. miltiorrhiza* proved effective for the treatment of CKD and CHF through various components, targets, and mechanisms. Moreover, it may predict the diagnostic value of key targets, providing a reference for clinical diagnostic applications.

IJKD 2025;19:69-83
www.ijkd.org
DOI: 10.52547/ijkd.7907

INTRODUCTION

Chronic kidney disease (CKD) has a global prevalence of 9.1%, with the number of affected people approaching 700 million and showing continuous increase.[1,2] Patients do not usually exhibit significant clinical symptoms during the early stages of the disease. However, in the late stages, patients may present with a range of symptoms, including anemia, bone mineral disorders, cognitive decline, and hypertension.[3]

Cardiovascular disease (CVD) has a profound impact on the condition and course of the disease in patients with CKD and is a major cause of disease recurrence and death in these patients.[4] Chronic heart failure (CHF) is considered the final stage of all types of CVD, often occurring in conjunction with CKD.[5] Studies have shown that the probability of comorbidity of the two diseases ranges from 31% to 39%.[6] The pathogenesis of both conditions is related to neurohormonal, hemodynamic, and inflammatory responses. Damage to one organ affects the health of the other, creating a vicious circle that eventually leads to an overall decrease in the function of both organs.[7] In terms of treatment, the dual effects on the heart and kidneys must be considered. Conventional drugs such as diuretics can effectively reduce cardiac load and relieve the symptoms of heart failure (HF) while improving renal function by lowering renal venous pressure. However, diuretic use can also lead to insufficient circulating blood volume and further aggravate cardiac and renal damage. Angiotensin-converting enzyme inhibitors and angiotensin receptor blockers can improve cardiac function, reduce proteinuria, and delay the progression of CKD but also have adverse effects such as decreased glomerular filtration rate and increased creatinine level.[8] Therefore, there is an urgent need to develop novel and effective treatments for CKD and CHF.

Chinese medicine has shown to have positive efficacy and advantages in treating CKD and CHF, and can effectively improve patients' clinical symptoms.[9,10] The Astragalus-Danshen drug pair is commonly used in the treatment of CKD and CHF.[11] Modern pharmacological studies have found that *Astragalus membranaceus* and *Salvia miltiorrhiza* inhibit pathological changes such as renal tubular swelling, peduncle fusion, and thylakoid hyperplasia in rats by regulating the PI3K/Akt and CAMKK/AMPK signaling pathways.[12] Corresponding clinical reports have shown that the combination of *A. membranaceus* and *S. miltiorrhiza* can reduce proteinuria, improve renal function, lower the risk of CKD-related mortality, and improve survival in CKD patients without the risk of hyperkalemia.[13,14] The bioactive components of Astragalus can inhibit the expressions of calcium-sensitive receptors and protein kinase C-α and improve cardiac diastolic function in rats with CHF, thus exerting an anti-myocardial fibrosis effect.[15] Danshen extract injection has been shown to have cardiovascular protective effects, inhibit ventricular hypertrophy, and improve cardiac function.[16] However, the molecular mechanism by which the Astragalus-Danshen drug pair plays a common role in CKD and CHF remains unclear.

In this study, we used a network pharmacology approach that ingredient bioinformatics, molecular docking, and kinetic simulations to conduct an in-depth analysis of the active components, targets, and mechanisms of the Astragalus-Danshen drug pair in the treatment of CKD and CHF. Using this methodology, we aimed to uncover the molecular mechanisms underlying the therapeutic action of the Astragalus-Danshen drug pair in these conditions.[18]

MATERIALS AND METHODS

Screening of active ingredients and targets of the Astragalus-Danshen drug pair

By using "Astragalus" and "Salvia miltiorrhiza" as keywords, Lipinski's rule[17] was used to search the TCMSP database,[18] relative molecular mass (MW) ≤ 500, lipid-water partition coefficient (AlogP) ≤ 5, number of hydrogen-bonded donors (Hdon) ≤ 5, and number of hydrogen-bonded acceptors (Hacc) ≤ 10. The screening criteria were oral bioavailability (OB) ≥ 30% and drug-likeness index (DL) ≥ 0.18.[19] The active ingredients and corresponding potential targets of *A. membranaceus* and *S. miltiorrhiza* were initially screened, combined, and deweighted by using the Uniprot database[20] and Perl. The targets were corrected and transformed into the corresponding human gene names to obtain the components and targets of the Astragalus-Danshen drug pair.

Screening for the CKD and CHF targets

The Gene Expression Omnibus (GEO) database[21] was searched and used to retrieve datasets GSE37171

and GSE66494 for CKD, and GSE21125 for CHF using "chronic kidney disease" and "chronic heart failure" as search terms. Data analysis was performed with the "SVA" and "limma" packages in R 4.2.0, applying multi-chip analysis with batch correction. The criteria for identifying differentially expressed genes were $|\log FC| > 1$ and $P < .05$.[19] In addition, disease targets were sourced from the GenCards,[22] OMIM,[23] TTD,[24] DisGeNET,[25] and Drug Bank[26] databases using the same search terms. Only targets with a relevance score 35 from the GenCards database were selected. After merging the data from all sources and removing duplicates, the list of targets for CKD and CHF was finalized.

Constructing a Network Linking the Active Ingredients of the Astragalus-Danshen Drug Pair to Common Therapeutic Targets in the Treatment of CKD and CHF

The drug and disease targets were uploaded to an online Venn diagram[27] to obtain the intersection genes of the drugs and diseases, and the drug, disease, and intersection targets were imported into Cytoscape 3.9.1.[28] The network was then constructed, and the top five core components were identified on the basis of the degree value (degree) of each node.

Construction of protein-protein interaction networks for the Astragalus-Danshen drug pair and intersection targets of CKD and CHF

Intersecting genes were imported into the STRING database.[29] The species were restricted to "*Homo sapiens*" on the interface. The protein-protein interaction (PPI) network was obtained by using the following criteria: highest confidence value of 0.9 and false discovery rate (FDR) stringency of 1%. The tab-separated values file was exported, and Cytoscape 3.9.1 was imported. The CytoNCA plug-in was used to construct a potential target network, with nodes representing individual targets and edges representing interactions among nodes, and to perform a systematic analysis of the network parameters.

Gene Ontology and Kyoto Encyclopedia of Genes and Genomes enrichment analyses

Gene Ontology (GO) enrichment analysis uses three parameters, namely biological process (BP), cellular component (CC), and molecular function (MF), to explain the biological processes of the intersecting genes, which are mainly designed to detect the major signaling pathways involved in the intersecting genes. Kyoto Encyclopedia of Genes and Genomes (KEGG) was designed to detect the major signaling pathways involved in gene intersections. In this study, the intersection targets were imported into the DAVID database[30] and the species was restricted to "*Homo sapiens*." FDRs < 0.01 were used for the GO and KEGG enrichment analyses.

Molecular docking

The five highest-ranked compounds from *A. membranaceus* and *S. miltiorrhiza* were selected for docking with the key targets. First, the structured data files of the three-dimensional (3D) structures of the compounds were downloaded from the PubChem database and converted to Protein Data Bank (PDB) format files using Open Babel 3.1.1. The 3D structures were then hydrogenated and calculated by using the AutoDockTools 1.5.6 software and saved as Protein Data Bank, Partial Charge, and Atom Type (PBDQT) files. Next, the protein structures of the targets were obtained from the Research Collaboratory for Structural Bioinformatics protein library[31] followed by dehydration, hydrogenation, and equilibrium charging of each target protein in AutoDockTools 1.5.6. The data obtained were then saved in the pdbqt format. Finally, molecular docking of the proteins to compound small molecules was performed by AutoDock Vina 1.1.2 and visualized by using PyMOL 2.6.0.

Molecular dynamics simulations

The stability and interaction of ligand binding to proteins were further evaluated by using the GROMACS 2019.4 package for 75-ns simulation runs. A Charmm36 force field was used to perform ligand topological transformation of the protein using the CGenFF server, followed by the generation of a TIP3P water model, neutralization of the charge of the system, and a 50,000-step energy minimization optimization. Then, in a 100-picosecond (ps) constant NVT (number of particles, volume, and temperature), the proteins were heated to 300 K. In constant NPT (number of particles, pressure, and temperature), maintaining the pressure at one standard atmosphere, an

equilibrium of 100-ps duration and 2-femtosecond (fs) time step was performed, during which the formation of atomic bonds was suppressed by using the LINear Constraint Solver algorithm. After the energy minimization and equilibration process, molecular dynamics simulations were performed with the Leap Frog algorithm for 75 nanoseconds (ns), with a time step of 2 fs, to determine the root mean square deviation (RMSD). Origin 2021 was used for visualization to understand the properties of the protein ligand.

Validation of the key target genes using ROC curves

ROC curves were plotted, and the area under the curve (AUC) values were calculated to evaluate the accuracy of the key genes for the diagnosis of CKD and CHF, using the R 4.2.0 "pROC" and "ggplot2" packages for network visualization.

RESULTS

Screening of active ingredients and drug targets

According to Lipinski's rule that OB and DL should be ≥30% and ≥0.18, respectively, 14 active ingredients and 432 targets from *A. membranaceus*, 56 active ingredients and 907 targets from *S. miltiorrhiza*, and 70 components were screened by using the TCMSP database. The 1339 targets were entered into the UniProt database to obtain the canonical names of the target genes, which were subsequently sorted and deleted by using the Perl language to obtain 191 targets for the action of the Astragalus-Danshen pair (Supplementary Table 1).

Target screening for diseases

Three microarray datasets (GSE37171, GSE66494, and GSE12215) from the GEO database were analyzed to identify 96 differentially expressed genes associated with CKD and 218 differentially expressed genes associated with CHF, and volcano and heat maps were constructed (Figure 1). In addition, we consolidate the disease targets for CKD and CHF by integrating data from the GenCards, OMIM, TTD, DisGeNet, and DrugBank databases aligning them with the GEO results; and eliminating duplicates, ultimately yielding 8018 targets for CKD and 5148 targets for CHF. We took the intersection of the disease targets and the Astragalus-Danshen drug-pair action, plotted a Venn diagram to obtain 158 intersection targets of the drugs and diseases (Figure 2). Specific information on the 158 intersection targets are presented in Supplementary Table 2.

Construction of a "drug-active component-common target disease" network

The two drugs, two diseases, 70 active ingredients, and 158 common targets were imported into the Cytoscape 3.9.1 software to construct the "drug active ingredient-common target-disease" network of the Astragalus-Dangshen drug pair for CKD and CHF interventions. Therefore, the network had 226 nodes and 1145 interaction lines, including 2 drug nodes, 2 disease nodes, 64 component nodes, and 158 common target nodes, with the yellow-pink triangle representing the drug, the V-shape representing the disease, the orange and green hexagons representing the main active ingredients of each drug, and the purple diamond node representing the common target, with the shade of color representing the degree size. The top 5 targets were quercetin, kaempferol, luteolin, tanshinone IIA, and 7-O-methylisomucronulatol (Table 1).

Construction of the protein-protein interaction and screening for the key targets

To unravel the mechanism underlying the therapeutic effect of the combination of *A. membranaceus* and *S. miltiorrhiza* in the treatment of CKD and CHF, 158 shared targets were integrated into the STRING database. Using a confidence score of 1.4 as the selection criterion, unrelated nodes were obscured, generating a protein-protein interaction (PPI) network (Figure 3B). Subsequently, we imported the PPI data into the Cytoscape 3.9.1 software and performed a topological analysis of the PPI network using the CytoNCA plugin. The median values of degree centrality (DC), closeness centrality (CC), and betweenness centrality (BC) were 7, 0.13, and 51.77, respectively. By establishing a selection condition in which DC, CC, and BC all exceeded their respective median values, we identified 44 key targets, which were then sorted in descending order of degree, which led to the identification of the top 5 key targets: protein kinase B1 (AKT1), signal transducer and activator of transcription 3 (STAT3), tumor protein P53 (TP53), mitogen-activated protein kinase 1 (MAPK1), and

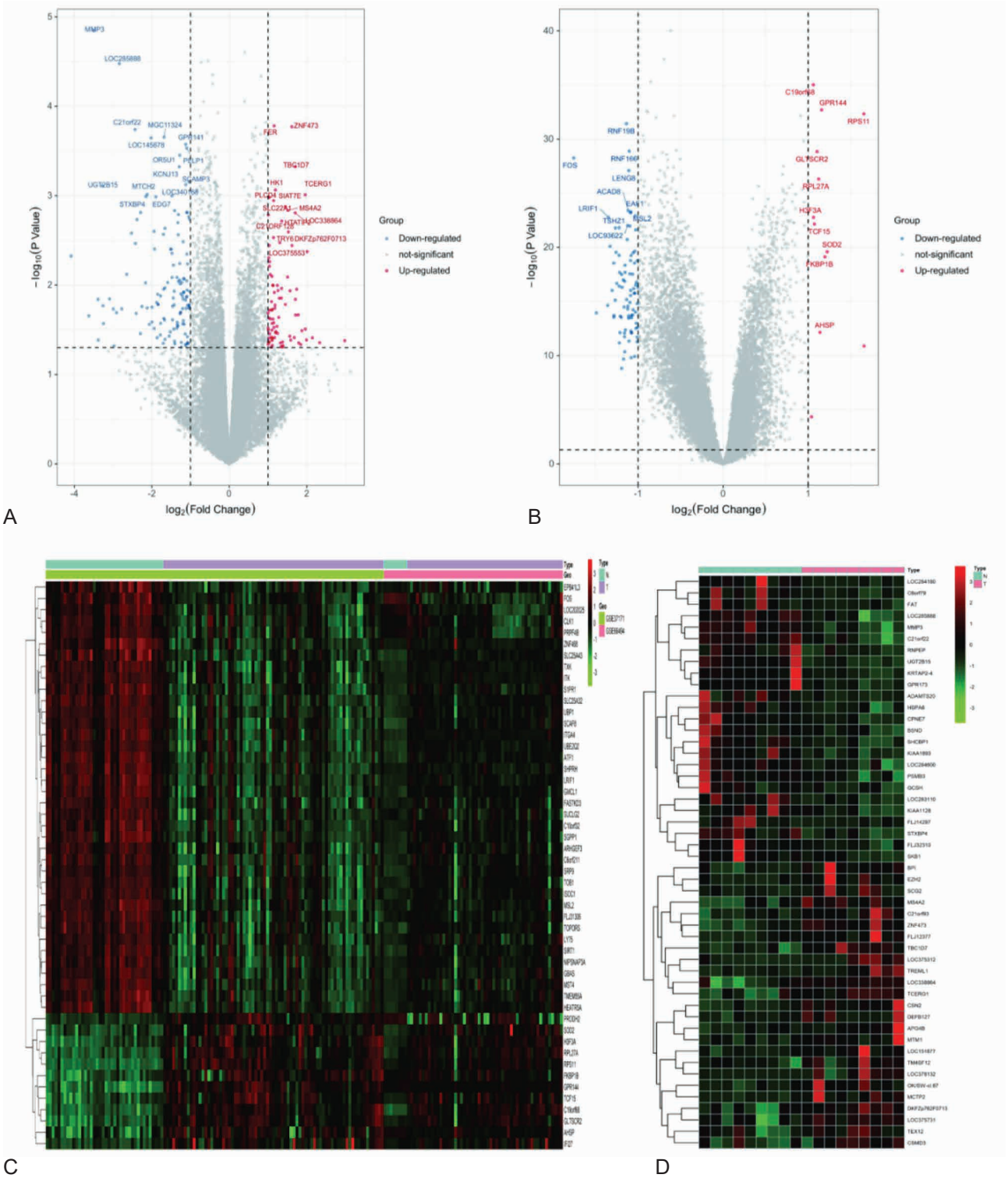

Figure 1. Volcano plots and heatmaps of CKD and CHF differential genes. (A) CKD differential gene volcano plot; (B) CHF differential gene volcano plot; (C) Top 50 heatmaps of CKD differential genes; (D) Top 50 heatmaps of CHF differential genes.

transcription factor p65 (RELA). In Figure 3C, a network comprised of 44 nodes and 252 edges is presented, with node color and size reflecting the degree values.

The GO and KEGG enrichment analysis of

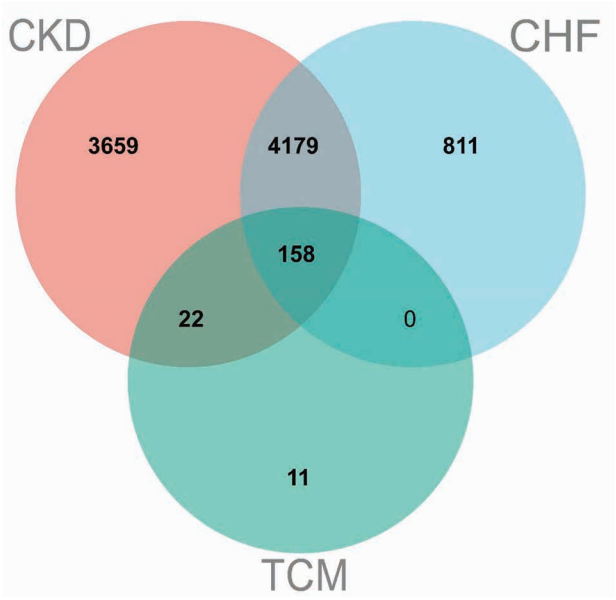

Figure 2. Venn diagram of the intersection targets of Traditional Chinese Medicine with CKD and CHF.

common targets

A total of 158 common targets were imported into the DAVID database, with a screening condition of FDR < 0.01. In the GO functional enrichment analysis, 192 entries were identified, including 412 BP-, 38 CC, and 85 MF-related entries. The top 10 entries in each of the BP, CC, and MF entries were selected on the basis of their FDR values using R 4.2.0. (Figure 4A), indicating that CKD and CHF involve complex biological processes, and that the Astragalus-Danshen drug pair can play a common regulatory role in CKD and CHF by regulating these biological processes. In addition, the analysis of the KEGG signaling pathways revealed that 162 signaling pathways were mapped to the intersection targets, and the top 20 pathways were selected in descending order of FDR value, mainly including pathways in cancer, the advanced glycosylation end products (AGE)-receptor for AGE (AGE-RAGE) signaling pathway in diabetic complications, lipid and atherosclerosis, fluid shear stress and atherosclerosis, the tumor necrosis factor (TNF) signaling pathway, the interleukin-17 (IL-17) signaling pathway, and the PI3K-Akt signaling pathway. The KEGG results also contained common signaling pathways that interfered with CKD and CHF, such as the p53, NF-Kappa B, and calcium signaling pathways. This suggests that *A. membranaceus* and *S. miltiorrhiza* interfered with the CKD and CHF processes through multiple targets and pathways.

Molecular docking and molecular dynamics simulations

Molecular docking of the core components quercetin, kaempferol, luteolin, tanshinone IIA, and 7-O-methylisomucronulatol, with the key targets AKT1, STAT3, TP53, MAPK1, and RELA, was performed. Binding energies £ 5.0 kcal/mol between two core components were considered to provide good binding activity, and ligand-receptor binding energies £ 7.0 kcal/mol were considered to have excellent binding activity.[31] The molecular docking results are shown in Table 2, where the binding energies of the core active ingredient to the key target were £6.0 kcal/mol. Some docking results were visualized by using PyMOL, as shown in Figure 5. Tanshinone IIA forms hydrogen bonds with AKT1, P53, and MAPK1 through the amino acids GLN-43, ARG-267, SER-99, LYS-162, and ASN-80. Quercetin forms hydrogen bonds with STAT3 via the amino acid residues LYS-370, ASP-396, and LEU-438. Luteolin forms hydrogen bonds with RELA through the amino acid residues GLN-20 and ARG-131. Molecular dynamics simulations provided insights into the stability of the protein-ligand complex. In this study, molecular dynamics simulations for quercetin-STAT3, tanshinone IIA-TP53, and tanshinone IIA-MAPK1 were performed for 75 ns based on docking results to assess molecular motions, trajectories, structural features, binding potentials, and conformational changes. The RMSD was used to assess the conformational stability of proteins and ligands, with smaller deviations indicating better conformational stability. Tanshinone IIA and quercetin were rapidly stabilized upon binding to their respective receptors, with RMSD fluctuations of < 0.2 nm. The results are shown in Figure 6.

Validation of the target genes using ROC curves

The ROC curves for the key genes, predicting the development of CKD and CHF, were plotted separately using R language (Figure 7). The AUC of the ROC curves ranged between 0.5 and 1, and the closer the AUC to 1, the better the diagnosis. As shown in Figure 7A, AKT1, TP53, and RELA showed high accuracy in their predictive abilities. STAT3 had some predictive accuracy, and MAPK1 had a low predictive accuracy. Figure 7B shows that AKT1

Table 1. Top 5 core components of Astragalus and Salvia Miltiorrhiza in treating CKD and CHF

Order number	ID	Active ingredient	Degree	Source
1	MOL000098	quercetin	111	Astragalus membranaceus
2	MOL000006	kaempferol	44	Astragalus membranaceus
3	MOL000422	luteolin	39	Salvia miltiorrhiza
4	MOL007154	tanshinone IIA	31	Salvia miltiorrhiza
5	MOL000378	7-O-methylisomucronulatol	25	Astragalus membranaceus

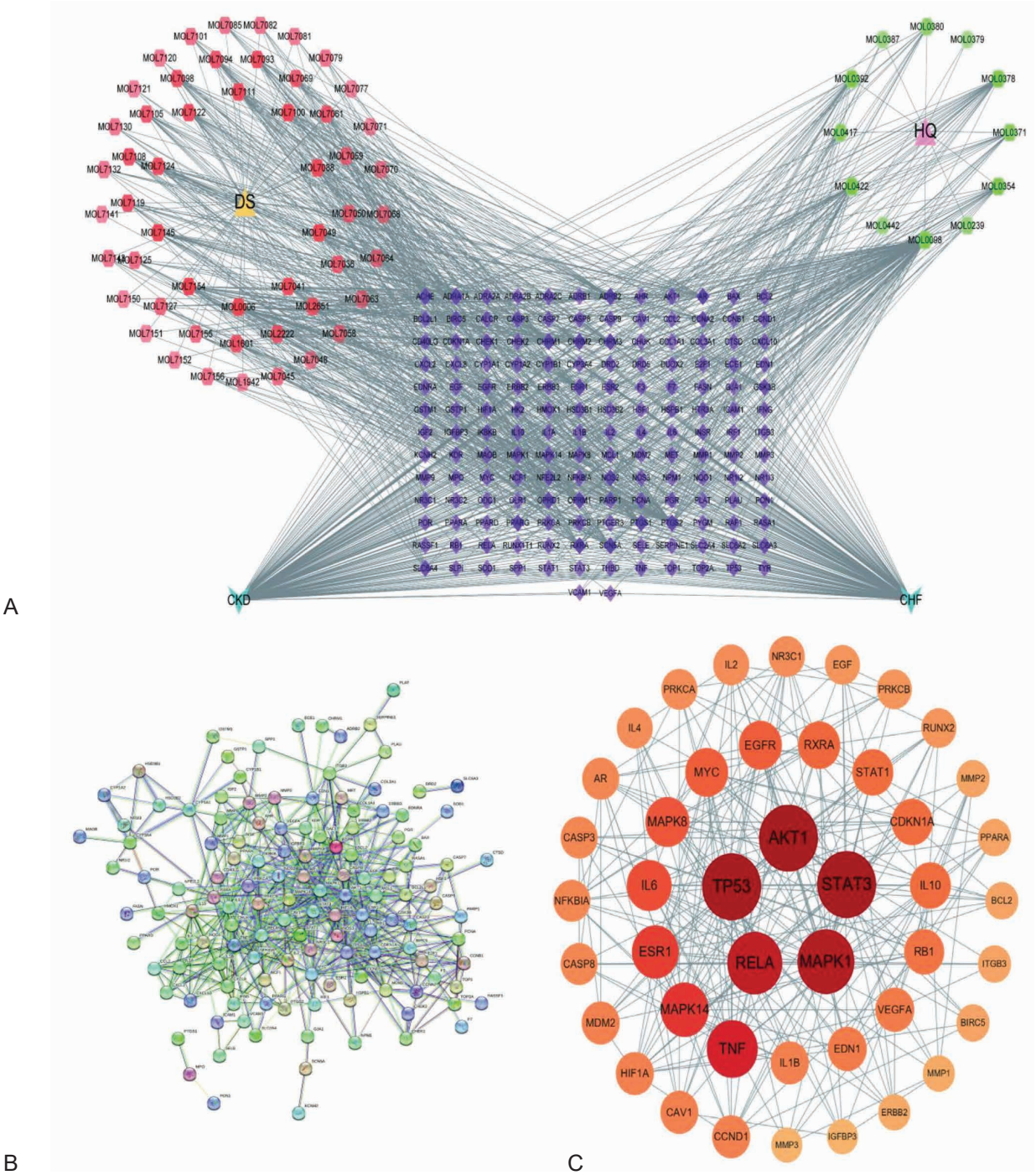

Figure 3. Astragalus membranaceus-Salvia miltiorrhiza Drug targets. (A) "Traditional Chinese medicine-active ingredient-intersectiontarget-disease" network of Astragalus membranaceus-Salvia miltiorrhiza drug pair. (B) PPI network of intersecting target proteins. (C) Core target network.

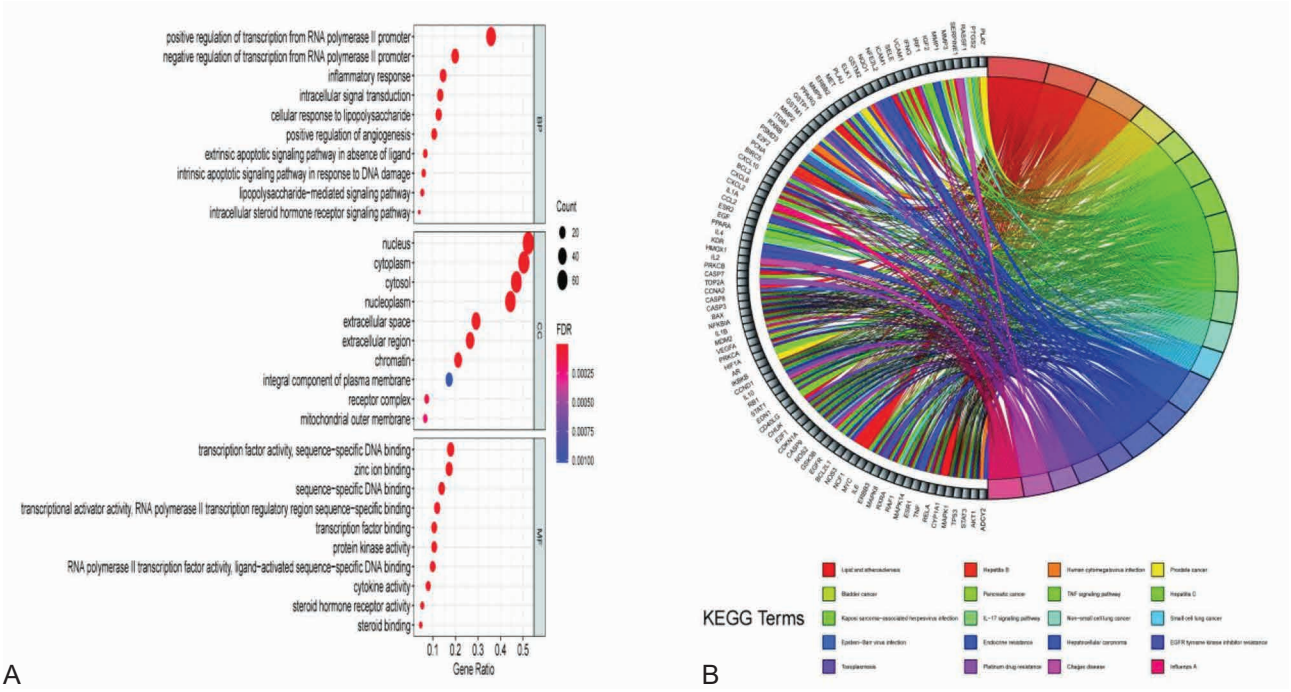

Figure 4. GO and KEGG enrichment analysis. (A) GO enrichment analysis of common targets. (B) KEGG enrichment analysis of common targets.

Table 2. Docking binding energy of core components and core targets

Key targets	PDB ID	Binding energy/ (kcal·mol^{-1})				
		Quercetin	Kaempferol	Luteolin	Tanshinone IIA	7-O-methylisomucronulatol
AKT1	1UNQ	-6.5	-6.1	-6.3	-6.9	-5.9
STAT3	6NJS	-8.1	-7.8	-7.9	-7.9	-6.8
TP53	3D06	-7.4	-6.9	-7.7	-7.9	-7.0
MAPK1	4ZZN	-7.3	-7.2	-7.4	-7.4	-6.4
RELA	6NV2	-7.2	-6.9	-7.3	-7.2	-6.5

and RELA had some predictive accuracy, STAT3 and MAPK1 had lower predictive accuracy, and TP53 had poor diagnostic efficacy. The predictive ability of the 5-gene combination showed high accuracy and higher AUC than those of the single genes, which had some clinical predictive value (Figure 7CD).

DISCUSSION

Chronic diseases such as CKD and CVD are becoming increasingly prevalent owing to development of human civilizations and the aging process.[32,33] These diseases share a common pathogenesis that leads to exacerbation and poor prognosis.[34] The treatment strategies for these diseases remain controversial, with no uniform standard. In Chinese medicine, the Astragalus-Dangshen drug pair is believed to be effective for the treatment of both diseases by improving microcirculation. Thus, we studied the targets and mechanisms of this drug pair in the treatment of different diseases.

The core active ingredients in this study were quercetin, kaempferol, luteolin, tanshinone IIA, and 7-O-methylisomucronulatol. Quercetin is a flavonoid believed to act on the PTEN/TIMP3, PI3K/Akt, TGF-β, and miR-124/NF-κB pathways, reducing macrophage accumulation and inflammatory cytokine expression in the kidney, exerting antioxidant effects, inhibiting inflammatory responses, and improving renal damage.[35] In recent years, dysbiosis of the gut flora has been identified as a risk factor for the progression of CKD, and the core theory of the "gut-kidney axis" suggests that dysbiosis of the gut flora can exacerbate urinary toxin accumulation; induce systemic microinflammatory

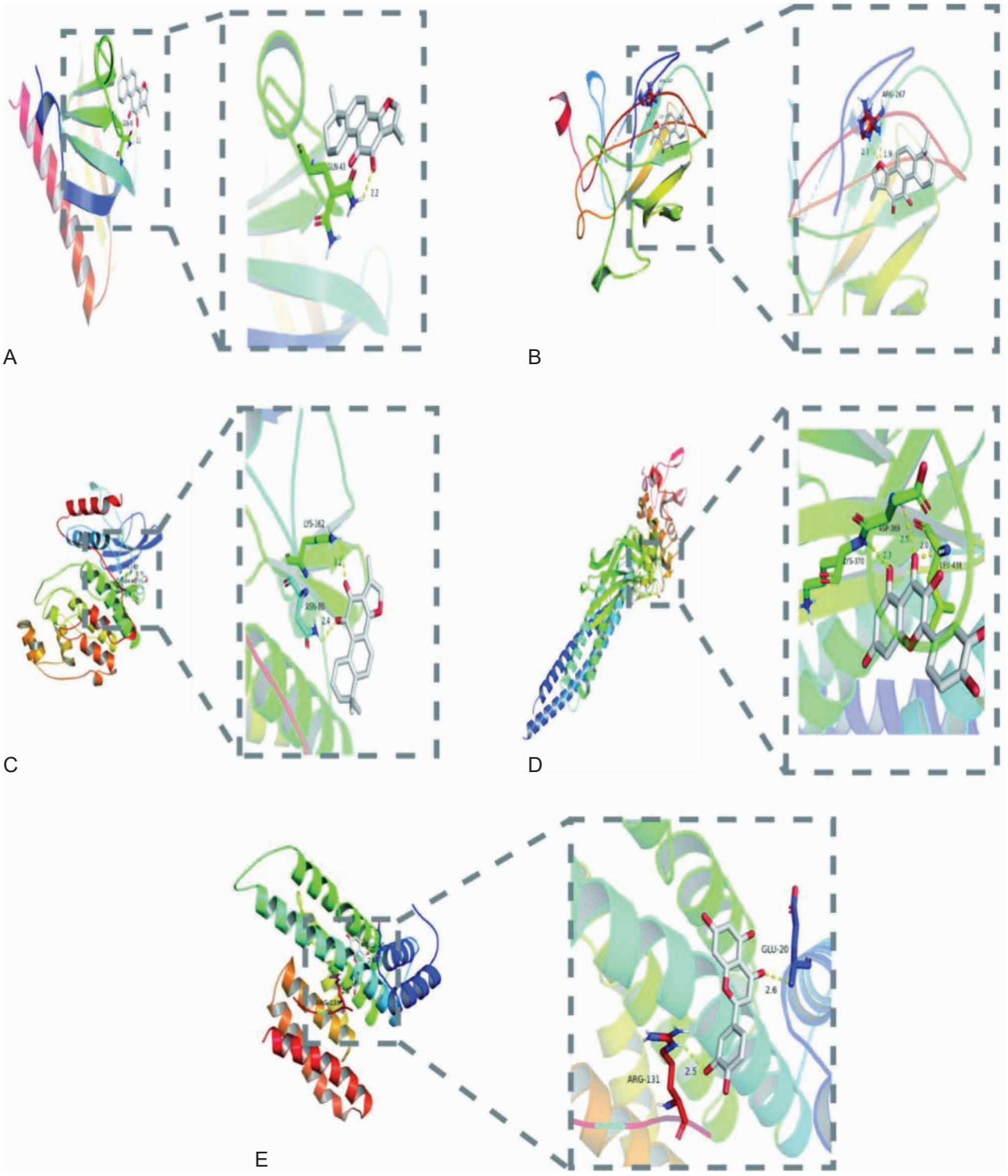

Figure 5. Molecular docking between core components (top 5) and core targets (top 5). (A) tanshinone IIA-AKT1. (B) tanshinone IIA-TP53. (C) tanshinone IIA-MAKT1. (D) quercetin-STAT3. (E) luteolin-RELA.

responses; aggravate kidney damage; inhibit the production of proinflammatory cytokines such as IL-17, TNF-α, and IL-6 in the gut; regulate intestinal microecology; and protect renal function.[36] In addition, quercetin significantly inhibits angiotensin II (Ang II)-induced myocardial fibrosis and has been

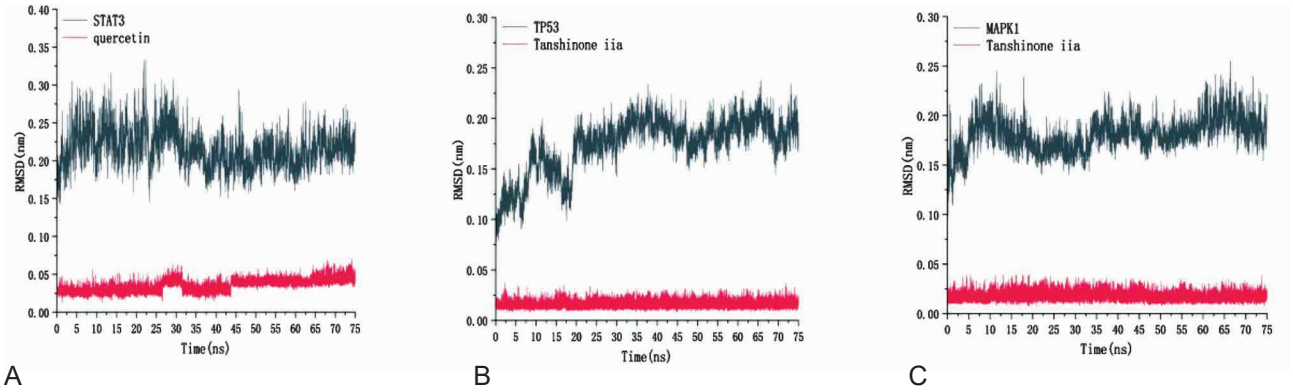

Figure 6. Molecular dynamics simulation of quercetin, tanshinone IIA, STAT3, TP53 and MAPK1. (A) quercetin-STAT3. (B) tanshinone IIA-TP53. (C) tanshinone IIA-MAPK1.

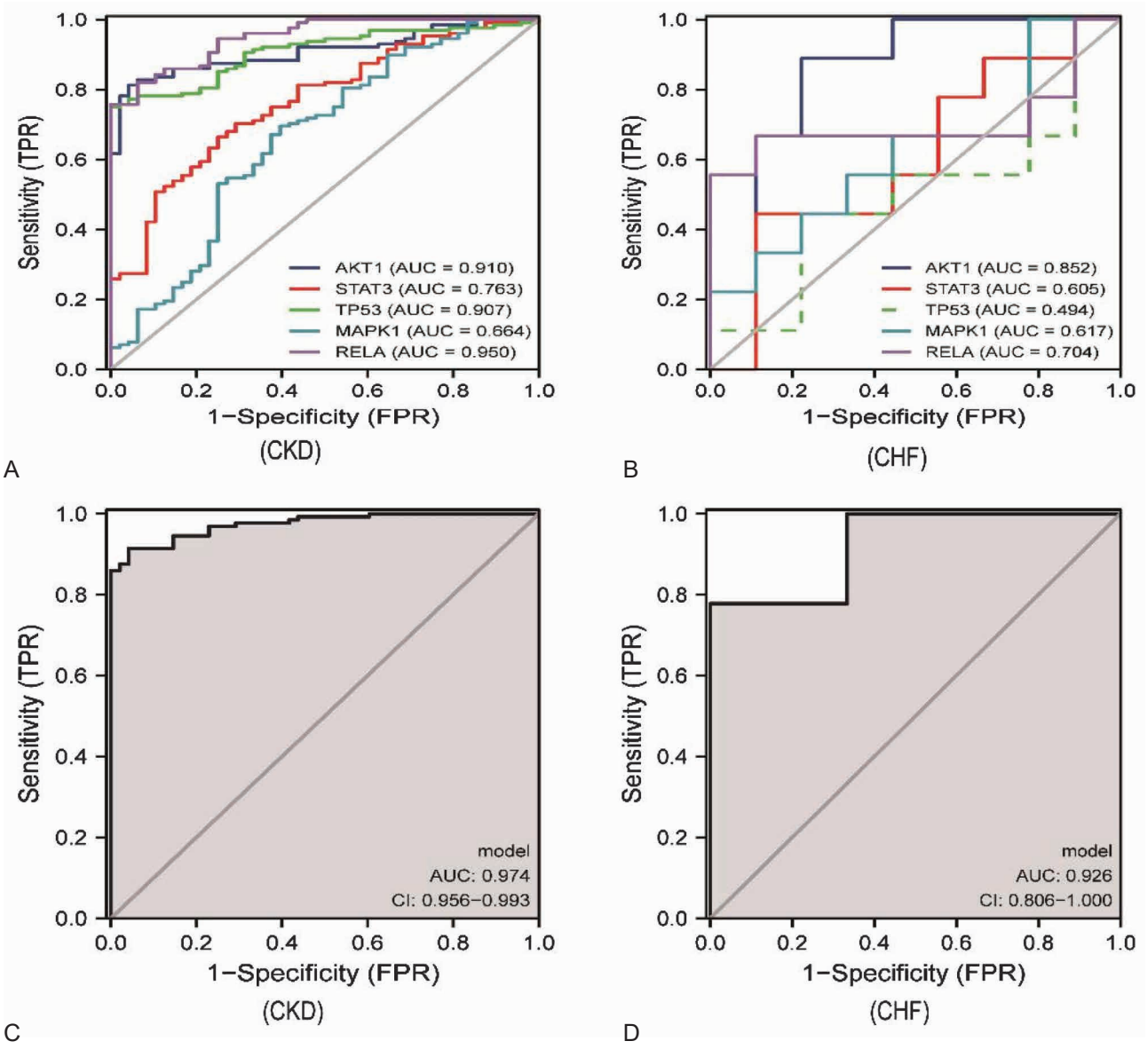

Figure 7. ROC curve of 5 core genes and their joint diagnosis.

shown to significantly improve myocardial injury both *in vivo* and *in vitro*.[37] Kaempferol has been shown to inhibit oxidative stress and inflammation in diabetic nephropathy, act as a nephroprotective agent, and exert a positive effect on cardiomyocytes by inhibiting apoptosis.[38,39]

During the progression of CKD, luteolin inhibits adriamycin-induced apoptosis in renal tubular epithelial cells by mediating MAPK phosphorylation and the p53 pathway.[40] Luteolin has also been shown to significantly increase the expression and activity of SERCA2a in sarcoplasmic reticulum Ca^{2+}-ATPase (SERSA) and to maintain intracellular Ca^{2+}.[41] Tanshinone IIA, the main lipophilic component of *S. miltiorrhiza*, protects against cardiac dysfunction.[42] In the kidney, it attenuates oxidative stress and endoplasmic reticulum stress-mediated apoptosis, prevents inflammation, and reduces glomerulosclerosis.[43]

The GO analysis results showed that the Astragalus-Danshen drug pair affected the positive regulation of RNA polymerase II promoter transcription, apoptosis, oxidative stress, and other BP; cytoplasm, plasma membrane, extracellular gap, and other CC; and protein binding, enzyme binding, and other MF. From the GO and KEGG analysis results, we found that the drug pair mainly exerted "allopathic" effects by participating in the regulation of the AGE-RAGE signaling pathway, TNF signaling pathway, lipid and atherosclerosis pathway, fluid shear stress and atherosclerosis, and IL-17 signaling pathway. AGEs are products of non-enzymatic glycosylation reactions between the amino portion of lysine and the reducing glyoxal group.[44] The formation of AGEs is closely associated with kidney failure[45] and plays a role in the pathogenesis of many CVDs.[46] The receptor for AGEs (RAGEs) is widely expressed in the heart and kidney, and its upregulated expression in many CVDs is associated with reduced cardiac function.[47] Blocking RAGE can improve cardiac function in patients with HF.[48] Lipid and shear stress can cause changes in the vascular wall, resulting in a local inflammatory environment.

Astragalus-Danshen drug pair acts on targets such as CCL2, AKT1, VCAM1, CHUK, NOS3, MAPK14, SELE, MMP9, IL1B, BCL2, TP53, and NFE2L2 to modulate the lipid and atherosclerotic pathways, fluid shear stress, and the arterial atherosclerotic pathways, and promote vascular remodeling.[49] TNF-α is an inflammatory factor and important mediator of renal fibrosis and HF, and increased TNF-α expression level in the kidney exacerbates angiotensin II-induced glomerular injury.[50] Studies have shown that TNF-α produced by myeloid cells induces proinflammatory differentiation of macrophages, triggers RIPK3-related necroptosis, and exacerbates renal loss and fibrosis.[51] The IL-17 family members include IL-17A, IL-17C, and IL-17E, with receptors such as IL-17RE, which play unique roles in inflammation and autoimmunity. IL-17- in TGF-β-induced renal fibroblast activation and extracellular matrix (ECM) synthesis exerts an inhibitory effect on renal interstitial fibrosis by decreasing P38MAPK and AKT phosphorylation.[52] The NF-κB transcription factor, a key event in IL-17 signaling, can be activated by IL-17A, downregulate SERCA2a and Cav1.2 expressions, and impair cardiomyocyte function contraction and structural remodeling.[53]

AKT1, STAT3, TP53, MAPK1, and RELA were identified as key targets. The docking results with the core components showed good binding ability between the compounds and the target proteins. On the basis of the network and docking results, combined with the biological significance of the targets in the literature and the safety of the components, the best binding proteins and ligands, namely quercetin-STAT3, tanshinone IIA-TP53, and tanshinone IIA-MAPK1, were selected for the molecular dynamics simulations. These simulations showed that the ligand- receptor complexes were tightly bound and rapidly reached a steady state. This suggests that the drug may mainly act on targets such as AKT1, STAT3, TP53, MAPK1, and RELA, which play an important role in improving CKD and CHF. AKT1 is an isoform of AKT that is closely related to cell proliferation, migration, and apoptosis. AKT1 deficiency promotes the expression of TGF-β1, fibrosis markers, and renal tubules, both *in vivo* and *in vitro*, and exacerbates the progression of CKD.[54] In the heart, AKT1 activation regulates cell size and survival, reduces apoptosis, and is beneficial for heart failure.[55]

The activation of STAT3, a member of the STATS family, resists cardiomyocyte apoptosis.[56] STAT3 activation in the ischemic and hypoxic heart has a protective effect, but sustained activation may have detrimental effects.[57] The inhibition of STAT3 activity in a CKD model ameliorated ECM

deposition and inflammatory cell infiltration.[58] TP53 encodes p53, which regulates the expressions of genes related to the cell cycle and senescence and is closely associated with human cancer. p53 knockdown was found to reduce endoplasmic reticulum stress and alter cardiac metabolism and cellular outcomes.[59] The role of p53 in CKD is controversial, and further research is required to determine whether TP53 and p53 can be used as treatment targets in CKD.[60]

ERK is a member of the mitogen-activated protein kinase (MAPK) family and has two isoforms: ERK1 (MAPK3) and ERK2 (MAPK1). Activation of ERK1 and ERK2 plays an important role in cell signaling, particularly by affecting the activity of its downstream factors, p65 and NF-κB. The regulation of these two activities is directly related to the proper kidney functioning.[61] In mouse models, cardiomyocyte-specific ERK2 deficiency has been observed to be associated with an increased incidence of HF. This suggests that ERK2 may play a crucial protective role in cardiomyocytes and that cardiomyocyte-specific ERK2 deficiency may disrupt cardiomyocyte endostasis, thereby increasing the risk of HF.[62] RelA (p65) is an important member of the NF-κB family and is associated with the classical activation pathway of NF-κB. The NF-κB signaling pathway is a major signaling pathway for inflammation and immunity that is directly involved in the development and progression of cardiac and renal inflammation.[63-66]

Subsequently, to evaluate the diagnostic value of the key genes for CKD and CHF in depth, we used ROC curves for prediction. The AUC of AKT1, STAT3, MAPK1, and RELA were all > 0.5, and the AUC of TP53 in CHF was 0.494, indicating the low diagnostic value of TP53 for CHF. However, after combining the key genes for diagnostic prediction, all AUC were > 0.9, which were superior to the AUC of the individual genes. This suggests that these five key genes have a high diagnostic value in differentiating patients with CKD and CHF from controls. However, further validation of their expressions and specific functions by immuno-infiltration analysis, mutation analysis, and real-time reverse transcription polymerase chain reaction is needed.

CONCLUSION

This study integrated bioinformatics technology, network pharmacology, molecular docking, kinetic simulation, and other methods. On the basis of the theory of "treating different diseases together," we preliminarily elucidated that the 70 active ingredients of the Astragalus-Danshen drug pair can act on 158 targets; regulate the AGE-RAGE, TNF, IL-17, and other signaling pathways; inhibit inflammation, oxidative stress, and apoptosis; and take advantage of the multi-component, multi-target, and multi-pathway benefits of Chinese medicine in the treatment of CKD and CHF. To a certain extent, this study provides a theoretical basis for the clinical application of Astragalus-Danshen drug pair. In this study, the drug database was screened according to various conditions but did not include information on the dose-effect relationships and interactions between drug components, which inevitably affected the results of this study to some extent. Therefore, a follow-up study should build on the present study to examine the exact relationship between the ingredients and use the intestinal flora as an entry point to conduct in-depth research on the effect of Chinese medicine interventions on diseases and validate the results in in-vitro experiments.

STATEMENTS & DECLARATIONS

Funding

This study was supported by the Fifth National Training Program for Outstanding Clinical Talents in Chinese Medicine (National Chinese Medicine Human Education Letter [2022] no. 1).

Competing Interests

The authors declare no conflict of interest.

Author Contributions

J.Q. conceived of and supervised the study. J.L. downloaded and analyzed the data. J.L. wrote the first draft of this manuscript. J.Q. was involved in the revision of the manuscript. All the authors approved the final manuscript.

Data Availability

The original contributions presented in this study are included in the article/Supplementary Material, and further inquiries can be directed to the corresponding author.

REFERENCES

1. Wang R, Hu B, Ye C, Zhang Z, Yin M, Cao Q, et al.

Stewed rhubarb decoction ameliorates adenine-induced chronic renal failure in mice by regulating gut microbiota dysbiosis. Frontiers in Pharmacology. 2022;13:842720.

2. Zhang R, Saredy J, Shao Y, Yao T, Liu L, Saaoud F, et al. End-stage renal disease is different from chronic kidney disease in upregulating ROS-modulated proinflammatory secretome in PBMCs-A novel multiple-hit model for disease progression. Redox biology. 2020;34:101460.
3. van den Brand JA, Mutsaers HA, van Zuilen AD, Blankestijn PJ, van den Broek PH, Russel FG, et al. Uremic solutes in chronic kidney disease and their role in progression. PLoS One. 2016;11(12):e0168117.
4. Tuttle KR, Brosius Iii FC, Cavender MA, et al. SGLT2 inhibition for CKD and cardiovascular disease in type 2 diabetes: report of a scientific workshop sponsored by the National Kidney Foundation. Diabetes. 2021;70(1):1–16.
5. Wang X, Li C, Gong H. Morphological and functional changes in bone marrow mesenchymal stem cells in rats with heart failure. Experimental and therapeutic medicine. 2017;13(6):2888-92.
6. McAlister FA, Ezekowitz J, Tonelli M, Armstrong PW. Renal insufficiency and heart failure: prognostic and therapeutic implications from a prospective cohort study. Circulation. 2004;109(8):1004-9.
7. Curaj A, Vanholder R, Loscalzo J, et al. Cardiovascular consequences of uremic metabolites: an overview of the involved signaling pathways. Circ Res. 2024;134(5):592–613.
8. Rangaswami J, Bhalla V, Blair JE, Chang TI, Costa S, Lentine KL, et al. Cardiorenal syndrome: classification, pathophysiology, diagnosis, and treatment strategies: a scientific statement from the American Heart Association. Circulation. 2019;139(16):e840-e78.
9. He X, Li G, Chen Y, Xiao Q, Yu X, Yu X, et al. Pharmacokinetics and pharmacodynamics of the combination of rhein and curcumin in the treatment of chronic kidney disease in rats. Frontiers in Pharmacology. 2020;11:573118.
10. Fan C, Tang X, Ye M, Zhu G, Dai Y, Yao Z, et al. Qi-Li-Qiang-Xin alleviates isoproterenol-induced myocardial injury by inhibiting excessive autophagy via activating AKT/mTOR pathway. Frontiers in Pharmacology. 2019;10:1329.
11. Ren C, Zhao X, Liu K, Wang L, Chen Q, Jiang H, et al. Research progress of natural medicine Astragalus mongholicus Bunge in treatment of myocardial fibrosis. Journal of Ethnopharmacology. 2023:116128.
12. Li W, Jiang Y-h, Wang Y, Zhao M, Hou G-j, Hu H-z, et al. Protective effects of combination of radix astragali and radix salviae miltiorrhizae on kidney of spontaneously hypertensive rats and renal intrinsic cells. Chinese Journal of Integrative Medicine. 2020;26:46-53.
13. Huang K-C, Su Y-C, Sun M-F, Huang S-T. Chinese herbal medicine improves the long-term survival rate of patients with chronic kidney disease in Taiwan: a nationwide retrospective population-based cohort study. Frontiers in Pharmacology. 2018;9:1117.
14. Chen Y-C, Chen H-T, Yeh C-C, Hung S-K, Yu B-H. Four prescribed Chinese herbal medicines provide renoprotection and survival benefit without hyperkalemia risk in patients with advanced chronic kidney disease: A nationwide cohort study. Phytomedicine. 2022;95:153873.
15. Li M, Han B, Zhao H, Xu C, Xu D, Sieniawska E, et al. Biological active ingredients of Astragali Radix and its mechanisms in treating cardiovascular and cerebrovascular diseases. Phytomedicine. 2022;98:153918.
16. Yuan T, Chen Y, Zhou X, Lin X, Zhang Q. Effectiveness and safety of Danshen injection on heart failure: protocol for a systematic review and meta-analysis. Medicine. 2019;98(22).
17. Lipinski CA, Lombardo F, Dominy BW, Feeney PJ. Experimental and computational approaches to estimate solubility and permeability in drug discovery and development settings. Advanced drug delivery reviews. 2012;64:4-17.
18. Ru J, Li P, Wang J, et al. TCMSP: a database of systems pharmacology for drug discovery from herbal medicines. J Cheminform. 2014;6:1–6.
19. Xu X, Zhang W, Huang C, Li Y, Yu H, Wang Y, et al. A novel chemometric method for the prediction of human oral bioavailability. International journal of molecular sciences. 2012;13(6):6964-82.
20. Uniprot Consortium. UniProt: the Universal Protein Knowledgebase in 2025. Nucleic Acids Res. 2025;53(D1):D609–17.
21. Barrett T, Wilhite SE, Ledoux P, et al. NCBI GEO: archive for functional genomics data sets—update. Nucleic Acids Res. 2012;41(D1):D991–5.
22. Stelzer G, Rosen N, Plaschkes I, et al. The GeneCards suite: from gene data mining to disease genome sequence analyses. Curr Protoc Bioinformatics. 2016;54(1):1–30.
23. Lee-Barber J, Kulo V, Lehmann H, Hamosh A, Bodurtha J. Bioinformatics for medical students: a 5-year experience using OMIM® in medical student educationGenet Med. 2019;21(2):493–7.
24. Zhou Y, Zhang Y, Zhao D, et al. TTD: therapeutic target database describing target druggability information. Nucleic Acids Res. 2024;52(D1):D1465–77.
25. Piñero J, Ramírez-Anguita JM, Saüch-Pitarch J, et al. The DisGeNET knowledge platform for disease genomics: 2019 update. Nucleic Acids Res. 2020;48(D1):D845–55.
26. Knox C, Wilson M, Klinger CM, et al. DrugBank 6.0: the DrugBank knowledgebase for 2024. Nucleic Acids Res. 2024;52(D1):D1265–75.
27. Bardou P, Mariette J, Escudié F, Djemiel C, Klopp C. jvenn: an interactive Venn diagram viewer. BMC Bioinformatics. 2014;15:1–7.
28. Shannon P, Markiel A, Ozier O, et al. Cytoscape: a software environment for integrated models of biomolecular interaction networks. Genome Res. 2003;13(11):2498–504.
29. Szklarczyk D, Kirsch R, Koutrouli M, et al. The STRING database in 2023: protein--protein association networks and functional enrichment analyses for any sequenced genome of interest. Nucleic Acids Res. 2023;51(D1):D638–46.
30. Sherman BT, Hao M, Qiu J, et al. DAVID: a web server for functional enrichment analysis and functional

annotation of gene lists (2021 update). Nucleic Acids Res. 2022;50(W1):W216–21.

31. Berman HM, Westbrook J, Feng Z, et al. The protein data bank. Nucleic Acids Res. 2000;28(1):235–42.
32. Hsin K-Y, Ghosh S, Kitano H. Combining machine learning systems and multiple docking simulation packages to improve docking prediction reliability for network pharmacology. PloS one. 2013;8(12):e83922.
33. Ould Setti M, Voutilainen A, Tuomainen TP. Renal hyperfiltration, fatty liver index, and the hazards of all-cause and cardiovascular mortality in Finnish men. Epidemiol Health. 2021;43:e2021001.
34. Hughes RL, Alvarado DA, Swanson KS, Holscher HD. The Prebiotic Potential of Inulin-Type Fructans: A Systematic Review. Adv Nutr. 2022;13(2):492–529.
35. Lai Y, Zhu Y, Zhang X, et al. Gut microbiota-derived metabolites: Potential targets for cardiorenal syndrome. Pharmacol Res. 2025;214:107672.
36. Chen Y-Q, Chen H-Y, Tang Q-Q, Li Y-F, Liu X-S, Lu F-H, et al. Protective effect of quercetin on kidney diseases: From chemistry to herbal medicines. Frontiers in Pharmacology. 2022;13:968226.
37. Dong Y, Lei J, Zhang B. Effects of dietary quercetin on the antioxidative status and cecal microbiota in broiler chickens fed with oxidized oil. Poultry science. 2020;99(10):4892-903.
38. Wang L, Tan A, An X, Xia Y, Xie Y. Quercetin dihydrate inhibition of cardiac fibrosis induced by angiotensin II in vivo and in vitro. Biomedicine & Pharmacotherapy. 2020;127:110205.
39. Sharma D, Gondaliya P, Tiwari V, Kalia K. Kaempferol attenuates diabetic nephropathy by inhibiting RhoA/Rho-kinase mediated inflammatory signalling. Biomedicine & Pharmacotherapy. 2019;109:1610-9.
40. Suchal K, Malik S, Khan SI, Malhotra RK, Goyal SN, Bhatia J, et al. Molecular pathways involved in the amelioration of myocardial injury in diabetic rats by kaempferol. International Journal of Molecular Sciences. 2017;18(5):1001.
41. Yong C, Zhang Z, Huang G, Yang Y, Zhu Y, Qian L, et al. Exploring the critical components and therapeutic mechanisms of Perilla frutescens L. in the treatment of chronic kidney disease via network pharmacology. Frontiers in pharmacology. 2021;12:717744.
42. Yan Q, Li Y, Yan J, Zhao Y, Liu Y, Liu S. Effects of luteolin on regulatory proteins and enzymes for myocyte calcium circulation in hypothermic preserved rat heart. Exp Ther Med. 2018;15(2):1433–41.
43. Wang X, Li C, Wang Q, Li W, Guo D, Zhang X, et al. Tanshinone IIA restores dynamic balance of autophagosome/autolysosome in doxorubicin-induced cardiotoxicity via targeting beclin1/LAMP1. Cancers. 2019;11(7):910.
44. Wang D-T, Huang R-H, Cheng X, Zhang Z-H, Yang Y-J, Lin X. Tanshinone IIA attenuates renal fibrosis and inflammation via altering expression of TGF-β/Smad and NF-κB signaling pathway in 5/6 nephrectomized rats. International immunopharmacology. 2015;26(1):4-12.
45. Taguchi K, Elias BC, Brooks CR, Ueda S, Fukami K. Uremic toxin–targeting as a therapeutic strategy for preventing cardiorenal syndrome. Circulation Journal. 2019;84(1):2-8.
46. Wang C-C, Lee A-S, Liu S-H, Chang K-C, Shen M-Y, Chang C-T. Spironolactone ameliorates endothelial dysfunction through inhibition of the AGE/RAGE axis in a chronic renal failure rat model. BMC nephrology. 2019;20(1):1-13.
47. Paradela-Dobarro B, Agra RM, Álvarez L, Varela-Román A, García-Acuña JM, González-Juanatey JR, et al. The different roles for the advanced glycation end products axis in heart failure and acute coronary syndrome settings. Nutrition, Metabolism and Cardiovascular Diseases. 2019;29(10):1050-60.
48. Neviere R, Yu Y, Wang L, Tessier F, Boulanger E. Implication of advanced glycation end products (Ages) and their receptor (Rage) on myocardial contractile and mitochondrial functions. Glycoconjugate journal. 2016;33:607-17.
49. Gao W, Zhou Z, Liang B, Huang Y, Yang Z, Chen Y, et al. Inhibiting receptor of advanced glycation end products attenuates pressure overload-induced cardiac dysfunction by preventing excessive autophagy. Frontiers in Physiology. 2018;9:1333.
50. Baeyens N, Bandyopadhyay C, Coon BG, Yun S, Schwartz MA. Endothelial fluid shear stress sensing in vascular health and disease. The Journal of clinical investigation. 2016;126(3):821-8.
51. Zhang J, Patel MB, Griffiths R, Mao A, Song Y-s, Karlovich NS, et al. Tumor necrosis factor-α produced in the kidney contributes to angiotensin II–dependent hypertension. Hypertension. 2014;64(6):1275-81.
52. Wen Y, Lu X, Ren J, Privratsky JR, Yang B, Rudemiller NP, et al. KLF4 in macrophages attenuates TNFα-mediated kidney injury and fibrosis. Journal of the American Society of Nephrology: JASN. 2019;30(10):1925.
53. Sun B, Wang H, Zhang L, Yang X, Zhang M, Zhu X, et al. Role of interleukin 17 in TGF-β signaling-mediated renal interstitial fibrosis. Cytokine. 2018;106:80-8.
54. Xue G-l, Li D-s, Wang Z-y, Liu Y, Yang J-m, Li C-z, et al. Interleukin-17 upregulation participates in the pathogenesis of heart failure in mice via NF-κB-dependent suppression of SERCA2a and Cav1. 2 expression. Acta Pharmacologica Sinica. 2021;42(11):1780-9.
55. Kim IY, Lee MY, Park MW, Seong EY, Lee DW, Lee SB, et al. Deletion of Akt1 promotes kidney fibrosis in a murine model of unilateral ureteral obstruction. BioMed Research International. 2020;2020.
56. Kapustian L, Kroupskaya I, Rozhko O, Bobyk V, Ryabenko D, Sidorik L. Akt1 expression and activity at different stages in experimental heart failure. Pathophysiology. 2014;21(2):147-51.
57. Eid RA, Alkhateeb MA, Eleawa S, Al-Hashem FH, Al-Shraim M, El-Kott AF, et al. Cardioprotective effect of ghrelin against myocardial infarction-induced left ventricular injury via inhibition of SOCS3 and activation of JAK2/STAT3 signaling. Basic research in cardiology. 2018;113:1-16.
58. Nural-Guvener H, Zakharova L, Feehery L, Sljukic S, Gaballa M. Anti-fibrotic effects of class I HDAC inhibitor, mocetinostat is associated with IL-6/Stat3 signaling in ischemic heart failure. International journal of molecular

sciences. 2015;16(5):11482-99.

59. Pang M, Ma L, Gong R, Tolbert E, Mao H, Ponnusamy M, et al. A novel STAT3 inhibitor, S3I-201, attenuates renal interstitial fibroblast activation and interstitial fibrosis in obstructive nephropathy. Kidney international. 2010;78(3):257-68.
60. Hoshino A, Mita Y, Okawa Y, Ariyoshi M, Iwai-Kanai E, Ueyama T, et al. Cytosolic p53 inhibits Parkin-mediated mitophagy and promotes mitochondrial dysfunction in the mouse heart. Nature communications. 2013;4(1):2308.
61. Wang J, Pan J, Li H, Long J, Fang F, Chen J, et al. lncRNA ZEB1-AS1 was suppressed by p53 for renal fibrosis in diabetic nephropathy. Molecular Therapy-Nucleic Acids. 2018;12:741-50.
62. Li Z, Xu K, Zhang N, Amador G, Wang Y, Zhao S, et al. Overexpressed SIRT6 attenuates cisplatin-induced acute kidney injury by inhibiting ERK1/2 signaling. Kidney international. 2018;93(4):881-92.
63. Ulm S, Liu W, Zi M, Tsui H, Chowdhury SK, Endo S, et al. Targeted deletion of ERK2 in cardiomyocytes attenuates hypertrophic response but provokes pathological stress induced cardiac dysfunction. Journal of Molecular and Cellular Cardiology. 2014;72:104-16.
64. Danilewicz M, Wągrowska-Danilewicz M. The immunoexpression of glomerular NF-κB in proteinuric patients with proliferative and non-proliferative glomerulopathies. Polish Journal of Pathology. 2013;64(2):78-83.
65. Katare PB, Bagul PK, Dinda AK, Banerjee SK. Toll-like receptor 4 inhibition improves oxidative stress and mitochondrial health in isoproterenol-induced cardiac hypertrophy in rats. Frontiers in immunology. 2017;8:719.
66. Ren Q, Guo F, Tao S, Huang R, Ma L, Fu P. Flavonoid fisetin alleviates kidney inflammation and apoptosis via inhibiting Src-mediated NF-κB p65 and MAPK signaling pathways in septic AKI mice. Biomedicine & Pharmacotherapy. 2020;122:109772.
67. Sun H-J, Xiong S-P, Cao X, Cao L, Zhu M-Y, Wu Z-Y, et al. Polysulfide-mediated sulfhydration of SIRT1 prevents diabetic nephropathy by suppressing phosphorylation and acetylation of p65 NF-κB and STAT3. Redox biology. 2021;38:101813.

*Correspondence to:
Jianguo Qin,
Department of Nephropathy, Dongfang Hospital, Beijing University of Chinese Medicine, Beijing 100078, China
Email: docqteamtg@126.com
Tel: +86-15810611070

Received August 2023
Accepted May 2024